Branching ratio and CP violation of $B\to\pi\pi$ decays in the perturbative QCD approach

Cai-Dian Lü*
Physics Department, Hiroshima University, Higashi-Hiroshima 739-8526, Japan

Kazumasa Ukai†
Physics Department, Nagoya University, Nagoya 464-8602, Japan

Mao-Zhi Yang‡
Physics Department, Hiroshima University, Higashi-Hiroshima 739-8526, Japan

(Received 24 April 2000; revised manuscript received 7 November 2000; published 6 March 2001)

We calculate the branching ratios and CP asymmetries for $B^0\to\pi^+\pi^-$, $B^+\to\pi^+\pi^0$, and $B^0\to\pi^0\pi^0$ decays, in a perturbative QCD approach. In this approach, we calculate nonfactorizable and annihilation type contributions, in addition to the usual factorizable contributions. We find that the annihilation diagram contributions are not very small as previously argued. Our result is in agreement with the measured branching ratio of $B\to\pi^+\pi^-$ by the CLEO Collaboration. With a non-negligible contribution from annihilation diagrams and a large strong phase, we predict a large direct CP asymmetry in $B^0\to\pi^+\pi^-$, and $\pi^0\pi^0$, which can be tested by the current running B factories.

DOI: 10.1103/PhysRevD.63.074009 PACS number(s): 13.25.Hw, 11.10.Hi, 12.38.Bx

I. INTRODUCTION

The charmless B decays have aroused more and more interest recently, since they are a good place to study CP violation and are also sensitive to new physics [1]. The factorization approach (FA) is applied to hadronic B decays and is generalized to decay modes that are classified in the spin of final states [2–4]. The FA gives predictions in terms of form factors and decay constants. Although the predictions of branching ratios agree well with experiments in most cases, there are still some theoretical points unclear. First, it relies strongly on the form factors, which cannot be calculated by the FA itself. Second, the generalized FA shows that the nonfactorizable contributions are important in a group of channels [3,4]. The reason for this large nonfactorizable contribution needs more theoretical study. Third, the strong phase, which is important for the CP violation prediction, is quite sensitive to the internal gluon momentum [5]. This gluon momentum is the sum of momenta of two quarks, which go into two different mesons. It is difficult to define exactly in the FA approach. To improve the theoretical predictions of the nonleptonic B decays, we try to improve the factorization approach, and explain the size of the nonfactorizable contributions in a new approach.

We shall take a specific channel $B\to\pi\pi$ as an example. The $B\to\pi\pi$ decays are responsible for the determination of the angle ϕ_2 in the unitarity triangle which have been studied in the factorization approach in detail [2–4]. The recent measurements of $B\to\pi^+\pi^-$ by the CLEO Collaboration attracted much attention for these kinds of decays [6]. The most recent theoretical study [7] attempted to compute the nonfactorizable diagrams directly. But it could not also predict the transition form factors of $B\to\pi$.

In this paper, we would like to study the $B\to\pi\pi$ decays in the perturbative QCD approach (PQCD) [8]. In the $B\to\pi\pi$ decays, the B meson is heavy, sitting at rest. It decays into two light mesons with large momenta. Therefore the light mesons are moving very fast in the rest frame of B meson. In this case, the short distance hard process dominates the decay amplitude. We shall demonstrate that the soft final state interaction is not important, since there is not enough time for the pions to exchange soft gluons. This makes the perturbative QCD approach applicable. With the final pions moving very fast, there must be a hard gluon to kick the light spectator quark d or u (almost at rest) in the B meson to form a fast moving pion (see Fig. 1). So the dominant diagram in this theoretical picture is that one hard gluon from the spectator quark connecting with the other quarks in the four quark operator of the weak interaction. Unlike the usual FA, where the spectator quark does not participate in the decay process in a major way, the hard part of the PQCD approach consists of six quarks rather than four. We thus call it six-quark operators or six-quark effective theory. Applying the six-quark effective theory to B meson exclusive decays, we need meson wave functions for the hadronization of quarks into mesons. Separating that nonperturbative dynam-

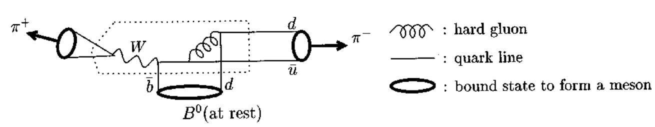

FIG. 1. One of the decay processes which contributes to $B\to\pi\pi$ decay. $\overline{b}$ quark decays to produce a fast moving $\overline{u}$ quark. In general, this quark and d quark are not lined up to form a pion. A gluon exchange is necessary in order that these quarks are lined up to form a pion. The part enclosed by dotted line describes the six-quark effective operator.

*Present address: Institute of High Energy Physics, P.O. Box 918(4), Beijing 100039, China. Email address: lucd@hptc5.ihep.ac.cn

†Email address: ukai@eken.phys.nagoya-u.ac.jp

‡Present address: Institute of High Energy Physics, P.O. Box 918(4), Beijing 100039, China. Email address: yangmz@hptc5.ihep.ac.cn

ics from the hard one, the decay amplitudes can be calculated in PQCD easily. Most of the nonperturbative dynamics are included in the meson wave functions, but in the correction that soft gluon straddle the six-quark operators, there are some nonfactorizable soft gluon effects not to be absorbed into the meson wave functions. Such effects can be safely neglected in the B meson decays [9].

Li performed the calculation of $\overline{B}^0 \to \pi^+\pi^-$ in Ref. [10] using the PQCD formalism, where the factorizable tree diagrams were calculated and the branching ratios were predicted. In another paper [11], Dahm, Jakob, and Kroll performed a more complete calculation, including the nonfactorizable annihilation topology and the three decay channels of $B \to \pi\pi$ decays. However, the predicted branching ratios are about one order smaller than the current experiments by CLEO [6]. In connection with this, Feldmann and Kroll concluded that perturbative contributions to the $B \to \pi$ transition form factor were much smaller than nonperturbative ones [12]. As we shall show later, the pion wave function must be consistent with chiral symmetry relation

$$-q^{\mu}\langle 0|\bar{u}\gamma_{\mu}\gamma_5 d(x)|\pi^-(q)\rangle = (m_u + m_d)\langle 0|\bar{u}\gamma_5 d(x)|\pi^-(q)\rangle. \tag{1}$$

This introduces terms that were not considered in the above calculations. In this paper, considering the terms needed from chiral symmetry, we calculate the $B \to \pi$ transition form factors and also the nonfactorizable contributions in the PQCD approach. We then show that our result for the branching ratio $B \to \pi^+\pi^-$ agrees with the measurement. Among the new terms, it is worthwhile emphasizing the presence of annihilation diagrams which are ignored in FA. We find that these diagrams cannot be ignored, and furthermore they contribute to large final state interaction phase.

II. THE FRAMEWORK

The three scale PQCD factorization theorem has been developed for nonleptonic heavy meson decays [13], based on the formalism by Brodsky and Lepage [14], and Botts and Sterman [15]. The QCD corrections to the four quark operators are usually summed by the renormalization group equation [16]. This has already been done to the leading logarithm and next-to-leading order for years. Since the b quark decay scale m_b is much smaller than the electroweak scale m_W, the QCD corrections are non-negligible. The third scale $1/b$ involved in the B meson exclusive decays is usually called the factorization scale, with b the conjugate variable of parton transverse momenta. The dynamics below $1/b$ scale is regarded as being completely nonperturbative, and can be parametrized into meson wave functions. The meson wave functions are not calculable in PQCD. But they are universal and channel independent. We can determine it from experiments, and it is constrained by QCD sum rules and lattice QCD calculations. Above the scale $1/b$, the physics is channel dependent. We can use perturbation theory to calculate channel by channel.

In addition to the hard gluon exchange with the spectator quark, the soft gluon exchanges between quark lines give out

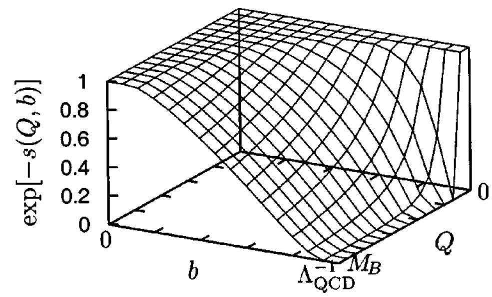

FIG. 2. b-Q dependence of e^{-s}. Nonperturbative region on $b \sim O(\Lambda^{-1})$ is suppressed by this exponent. Since the pion wave function has two Sudakov factor accompanied with two light quarks, this suppression becomes much stronger.

the double logarithms $\ln^2(Pb)$ from the overlap of collinear and soft divergences, P being the dominant light-cone component of a meson momentum. The resummation of these double logarithms leads to a Sudakov form factor $\exp[-s(P,b)]$, which suppresses the long distance contributions in the large b region, and vanishes as $b > 1/\Lambda_{QCD}$. This form factor is given to sum the leading order soft gluon exchanges between the hard part and the wave functions of mesons. So this term includes the double infrared logarithms. The expression of $s(Q,b)$ is concretely given in Appendix B. Figure 2 shows that e^{-s} falls off quickly in the large b, or long-distance, region, giving so-called Sudakov suppression. This Sudakov factor practically makes PQCD approach applicable. For the detailed derivation of the Sudakov form factors, see Refs. [8,17].

With all the large logarithms resummed, the remaining finite contributions are absorbed into a perturbative b quark decay subamplitude $H(t)$. Therefore the three scale factorization formula is given by the typical expression

$$C(t)\times H(t)\times\Phi(x) \times\exp\left[-s(P,b)-2\int_{1/b}^{t}\frac{d\bar{\mu}}{\bar{\mu}}\gamma_q[\alpha_s(\bar{\mu})]\right], \tag{2}$$

where $C(t)$ are the corresponding Wilson coefficients, $\Phi(x)$ are the meson wave functions and the variable t denotes the largest mass scale of hard process H, that is, six-quark effective theory. The quark anomalous dimension $\gamma_q = -\alpha_s/\pi$ describes the evolution from scale t to $1/b$. Since logarithm corrections have been summed by renormalization group equations, the above factorization formula does not depend on the renormalization scale μ explicitly.

The three scale factorization theorem in Eq. (2) is discussed by Li *et al.* in detail [13]. In Sec. III, we shall give the factorization formulas for $B \to \pi\pi$ decay amplitudes by calculating the hard part $H(t)$, channel dependent in PQCD. We shall also approximate H there by the $\mathcal{O}(\alpha_s)$ expression, which makes sense if perturbative contributions indeed dominate.

In the resummation procedures, the B meson is treated as a heavy-light system. The wave function is defined as

$$\Phi_B=\frac{1}{\sqrt{2N_c}}(\not p_B+m_B)\gamma_5\phi_B(k_1,k_b), \tag{3}$$

where $N_c=3$ is color's degree of freedom and $\phi_B(k_1,k_b)$ is the distribution function of the four-momenta of the light quark (k_1) and b quark (k_b)

$$\phi_B(k_1,k_b)=\frac{1}{p_B^2}\frac{1}{2\sqrt{2N_c}}\int\frac{d^4y}{(2\pi)^4}e^{ik_1\cdot y}\times\langle 0|\mathrm{T}[\overline{d}(y)\not p_B\gamma_5 b(0)]|B(p_B)\rangle. \tag{4}$$

Note that we use the same distribution function $\phi_B(k_1,k_b)$ for the $\not p_B$ term and the m_B term from heavy quark effective theory. For the hard part calculations in the next section, we use the approximation $m_b\simeq m_B$, which is the same order approximation neglecting higher twist of $(m_B-m_b)/m_B$. To form a bound state of B meson, the condition $k_b=p_B-k_1$ is required. So ϕ_B is actually a function of k_1 only. Throughout this paper, we take $p^\pm=(p^0\pm p^3)/\sqrt{2}$, $\mathbf{p}_T=(p^1,p^2)$ as the light-cone coordinates to write the four momentum. We consider the B meson at rest, then that momentum is $p_B=(m_B/\sqrt{2})(1,1,\mathbf{0}_T)$. The momentum of the light valence quark is written as $(k_1^+,k_1^-,\mathbf{k}_{1T})$, where the $\mathbf{k}_{1T}$ is a small transverse momentum. It is difficult to define the function $\phi_B(k_1^+,k_1^-,\mathbf{k}_{1T})$. However, in the next section, we will see that the hard part is always independent of k_1^+, if we make some approximations. This means that k_1^+ can be integrated out in Eq. (4), the function $\phi_B(k_1^+,k_1^-,\mathbf{k}_{1T})$ can be simplified to

$$\begin{aligned}\phi_B(x_1,\mathbf{k}_{1T})&=p_B^-\int dk_1^+\phi_B(k_1^+,k_1^-,\mathbf{k}_{1T})\\&=\frac{p_B^-}{p_B^2}\frac{1}{2\sqrt{2N_c}}\int\frac{dy^+d^2\mathbf{y}_T}{(2\pi)^3}e^{i(k_1^-y^+-\mathbf{k}_{1T}\cdot\mathbf{y}_T)}\\&\quad\times\langle 0|\mathrm{T}[\overline{d}(y^+,0,\mathbf{y}_T)\not p_B\gamma_5 b(0)]|B(p_B)\rangle,\end{aligned} \tag{5}$$

where $x_1=k_1^-/p_B^-$ is the momentum fraction. Therefore, in the perturbative calculations, we do not need the information of all four momentum k_1. The above integration can be done only when the hard part of the subprocess is independent of the variable k_1^+.

The π meson is treated as a light-light system. At the B meson rest frame, pion is moving very fast. We define the momentum of the pion which contains the spectator light quark as $P_2=(m_B/\sqrt{2})(1,0,\mathbf{0}_T)$. The other pion which moves to the inverse direction, then has momentum $P_3=(m_B/\sqrt{2})(0,1,\mathbf{0}_T)$. The light spectator quark moving with the pion (with momentum P_2), has a momentum $(k_2^+,0,\mathbf{k}_{2T})$. The momentum of the other valence quark in this pion is then $(P_2^+-k_2^+,0,-\mathbf{k}_{2T})$. If we define the momentum fraction as $x_2=k_2^+/P_2^+$, then the wave function of pion can be written as

$$\Phi_\pi=\frac{1}{\sqrt{2N_c}}\gamma_5[\not p_\pi\phi_\pi(x_2,\mathbf{k}_{2T})+m_0\phi'_\pi(x_2,\mathbf{k}_{2T})], \tag{6}$$

where $\phi_\pi(x_2,\mathbf{k}_{2T})$ is defined in analogy to Eqs. (4), (5) and $\phi'_\pi(x_2,\mathbf{k}_{2T})$ is defined by

$$\phi'_\pi(x_2,\mathbf{k}_{2T})=\frac{P_2^+}{2\sqrt{2N_c}}\int\frac{dy^-d^2\mathbf{y}_T}{(2\pi)^3}e^{i(x_2P_2^+y^--\mathbf{k}_{2T}\cdot\mathbf{y}_T)}\times\langle 0|\mathrm{T}[\overline{d}(0)\gamma_5 u(0,y^-,\mathbf{y}_T)]|\pi(P_2)\rangle. \tag{7}$$

Note that as you shall see below, m_0 given as

$$m_0=\frac{m_\pi^2}{m_u+m_d} \tag{8}$$

in Eq. (6) *is not* the pion mass. Since this m_0 is estimated around 1–2 GeV using the quark masses predicted from lattice simulations, one may guess contributions of m_0 term cannot be neglected because of $m_0\not\ll m_B$. In fact, we will show this m_0 plays important roles to predict the $B\to\pi\pi$ branching ratios in Sec. IV.

The normalization of wave functions is determined by meson's decay constant

$$\langle 0|\overline{d}(0)\gamma_\mu\gamma_5 u(0)|\pi(p)\rangle=ip_\mu f_\pi. \tag{9}$$

Using this relation, the normalization of ϕ_π is defined as

$$\int dx_2 d^2\mathbf{k}_{2T}\phi_\pi(x_2,\mathbf{k}_{2T})=\frac{f_\pi}{2\sqrt{2N_c}}. \tag{10}$$

Moreover, from Eq. (9) you can readily derive

$$\langle 0|\overline{d}(0)\gamma_5 u(0)|\pi(p)\rangle=-i\frac{m_\pi^2}{m_u+m_d}f_\pi, \tag{11}$$

so defining m_0 such as Eq. (8), the normalization of ϕ'_π is the same one to Eq. (10).

The transverse momentum $\mathbf{k}_T$ is usually conveniently converted to the b parameter by Fourier transformation. The initial conditions of $\phi_i^{(\prime)}(x)$, $i=B$, π, are of nonperturbative origin, satisfying the normalization

$$\int_0^1\phi_i^{(\prime)}(x,b=0)dx=\frac{f_i}{2\sqrt{2N_c}}, \tag{12}$$

with f_i the meson decay constants.

III. PERTURBATIVE CALCULATIONS

With the above brief discussion, the only thing left is to compute H for each diagram. There are altogether eight diagrams contributing to the $B\to\pi\pi$ decays, which are shown in Fig. 3. They are the lowest order diagrams. In fact the diagrams without hard gluon exchange between the spectator quark and other quarks are suppressed by the wave functions. The reason is that the light quark in B meson is almost at rest. If there is no large momentum exchange with other quarks, it carries almost zero momentum in the fast moving π, that is the end point of pion wave function. In the next

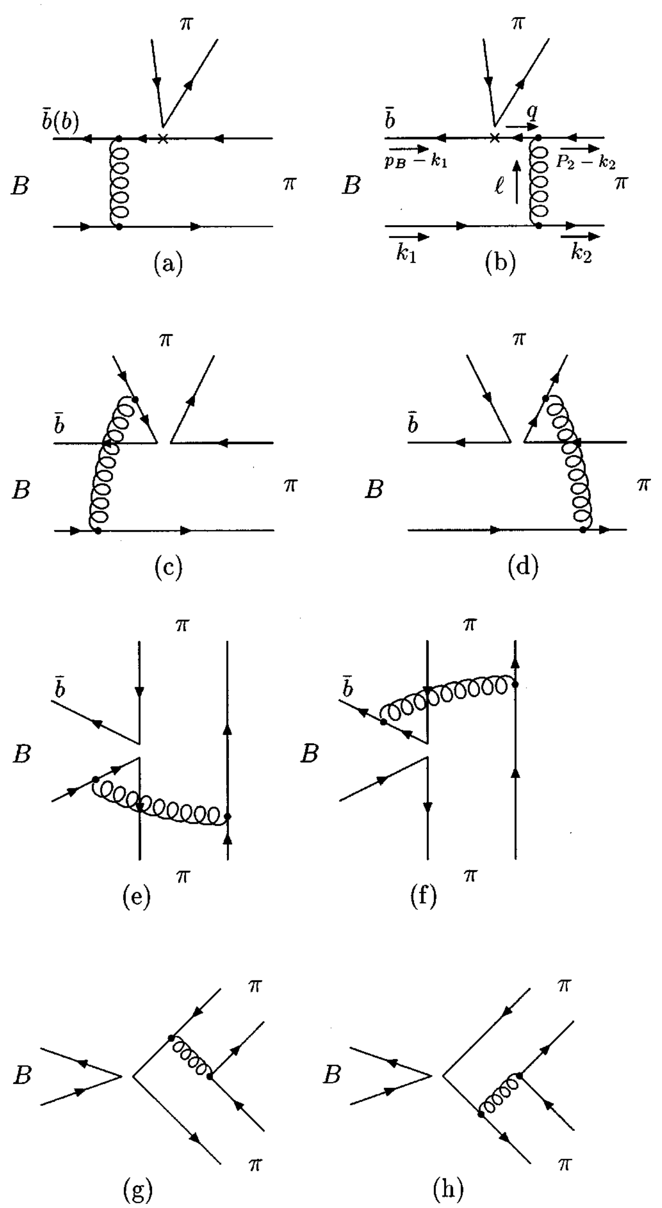

FIG. 3. Diagrams contributing to the $B\rightarrow\pi\pi$ decays. The diagram (b) corresponds to Fig. 1.

section, we will see that the pion wave function at the zero point is always zero. The Sudakov form factor suppresses the large number of soft gluons exchange to transfer large momentum. It is already shown that the hard gluon is really hard in the numerical calculations of $B\rightarrow K\pi$ [18]. The value of α_s/π is peaked below 0.2. And in our following calculation of $B\rightarrow\pi\pi$ decays this is also proved.

Let us first calculate the usual factorizable diagrams (a) and (b). The four quark operators indicated by a cross in the diagrams are shown in the Appendix A. There are two kinds of operators. Operators O_1, O_2, O_3, O_4, O_9, and O_{10} are $(V-A)(V-A)$ currents, the sum of their amplitudes is given as

$$
\begin{aligned}
F_e=&-16\pi C_F m_B^2\int_0^1 dx_1dx_2\int_0^\infty b_1db_1b_2db_2\,\phi_B(x_1,b_1)\\
&\times\{[(1+x_2)\phi_\pi(x_2,b_2)+(1-2x_2)\phi_\pi'(x_2,b_2)r_\pi]\\
&\times\alpha_s(t_e^1)h_e(x_1,x_2,b_1,b_2)\exp[-S_B(t_e^1)-S_\pi^1(t_e^1)]\\
&+2r_\pi\phi_\pi'(x_2,b_2)\alpha_s(t_e^2)h_e(x_2,x_1,b_2,b_1)\\
&\times\exp[-S_B(t_e^2)-S_\pi^1(t_e^2)]\},
\end{aligned}
\tag{13}
$$

where $r_\pi=m_0/m_B=m_\pi^2/[m_B(m_u+m_d)]$. $C_F=4/3$ is a color factor. The function $h_e(x_1,x_2,b_1,b_2)$ and the Sudakov form factors $S_B(t_i)$ and $S_\pi(t_i)$ are given in Appendix B. The operators O_5, O_6, O_7, and O_8 have a structure of $(V-A)(V+A)$. The sum of their amplitudes is

$$
\begin{aligned}
F_e^P=&-32\pi C_F m_B^2 r_\pi\int_0^1 dx_1dx_2\int_0^\infty b_1db_1b_2db_2\,\phi_B(x_1,b_1)\\
&\times\{[\phi_\pi(x_2,b_2)+(2+x_2)\phi_\pi'(x_2,b_2)r_\pi]\\
&\times\alpha_s(t_e^1)h_e(x_1,x_2,b_1,b_2)\exp[-S_B(t_e^1)-S_\pi^1(t_e^1)]\\
&+[x_1\phi_\pi(x_2,b_2)+2(1-x_1)\phi_\pi'(x_2,b_2)r_\pi]\\
&\times\alpha_s(t_e^2)h_e(x_2,x_1,b_2,b_1)\exp[-S_B(t_e^2)-S_\pi^1(t_e^2)]\}.
\end{aligned}
\tag{14}
$$

They are proportional to the factor r_π. There are also factorizable annihilation diagrams (g) and (h), where the B meson can be factored out. For the $(V-A)(V-A)$ operators, their contributions always cancel between diagram (g) and (h). But for the $(V-A)(V+A)$ operators, their contributions are sum of diagram (g) and (h).

$$
\begin{aligned}
F_a^P=&-64\pi C_F m_B^2 r_\pi\int_0^1 dx_2dx_3\int_0^\infty b_2db_2b_3db_3\alpha_s(t_a)\\
&\times h_a(x_2,x_3,b_2,b_3)[2\phi_\pi(x_2,b_2)\phi_\pi'(x_3,b_3)\\
&+x_2\phi_\pi(x_3,b_3)\phi_\pi'(x_2,b_2)]\exp[-S_\pi^1(t_a)-S_\pi^2(t_a)],
\end{aligned}
\tag{15}
$$

These two diagrams can be cut in the middle of the diagrams. They provide the main strong phase for nonleptonic B decays. Note that F_a^P vanishes in the limit of $m_0=0$. So the m_0 term in the pion wave function does not only have much effect on the branching ratios, but also the CP asymmetries. In addition to the factorizable diagrams, we can also calculate the nonfactorizable diagrams (c) and (d) and also the nonfactorizable annihilation diagrams (e) and (f). In this case, the amplitudes involve all three meson wave functions. The integration over b_3 can be performed easily using δ function $\delta(b_3-b_1)$ in diagrams (c),(d) and $\delta(b_3-b_2)$ for diagrams (e),(f).

$$\mathcal{M}_e=\frac{32}{3}\pi C_F\sqrt{2N_c}m_B^2\int_0^1 dx_1dx_2\,dx_3\int_0^\infty b_1db_1b_2db_2 \times\phi_B(x_1,b_1)\phi_\pi(x_2,b_2) \times\phi_\pi(x_3,b_1)x_2\alpha_s(t_d)h_d(x_1,x_2,x_3,b_1,b_2) \times\exp[-S_B(t_d)-S_\pi^1(t_d)-S_\pi^2(t_d)], \tag{16}$$

$$\mathcal{M}_a=\frac{32}{3}\pi C_F\sqrt{2N_c}m_B^2\int_0^1 dx_1dx_2\,dx_3\int_0^\infty b_1db_1b_2db_2 \times\phi_B(x_1,b_1)\{-[x_2\phi_\pi(x_2,b_2)\phi_\pi(x_3,b_2) +(x_2+x_3)\phi_\pi'(x_2,b_2)\phi_\pi'(x_3,b_2)r_\pi^2] \times\alpha_s(t_f^1)h_f^{(1)}(x_1,x_2,x_3,b_1,b_2)\exp[-S_B(t_f^1) -S_\pi^1(t_f^1)-S_\pi^2(t_f^1)]+[x_2\phi_\pi(x_2,b_2)\phi_\pi(x_3,b_2) +(2+x_2+x_3)\phi_\pi'(x_2,b_2)\phi_\pi'(x_3,b_2)r_\pi^2] \times\alpha_s(t_f^2)h_f^{(2)}(x_1,x_2,x_3,b_1,b_2)] \times\exp[-S_B(t_f^2)-S_\pi^1(t_f^2)-S_\pi^2(t_f^2)]\}. \tag{17}$$

Note that when doing the above integrations over x_i and b_i, we have to include the corresponding Wilson coefficients C_i evaluated at the corresponding scale t_i. The expression of Wilson coefficients are channel dependent which are shown later in this section. The functions h_i, coming from the Fourier transform of H, are given in Appendix B. In the above equations, we have used the assumption that $x_1\ll x_2,x_3$. Since the light quark momentum fraction x_1 in B meson is peaked at the small region, while quark momentum fraction x_2 of pion is peaked at 0.5, this is not a bad approximation. After using this approximation, all the diagrams are functions of $k_1^-=x_1m_B/\sqrt{2}$ of B meson only, independent of the variable of k_1^+. For example, by calculating the diagrams (b) we shall demonstrate it.

$$\begin{aligned}\langle\pi(P_2)\pi(P_3)|O_2^{u\dagger}|B(p_B)\rangle &\propto\int d^4k_1d^4k_2\phi_B(k_1)\phi_\pi'(k_2)\;\frac{q\cdot P_3}{q^2\,l^2}\\ &=\int d^4k_1d^4k_2\phi_B(k_1)\phi_\pi'(k_2)\times\frac{(P_2^+-k_1^+)p_B^-}{\{2(P_2^+-k_1^+)k_1^-+\mathbf{k}_{1T}^2\}\{2(k_2^+-k_1^+)k_1^-+l_T^2\}}\\ &\simeq\int d^4k_1d^4k_2\phi_B(k_1)\phi_\pi'(k_2)\times\left\{\frac{p_B^-P_2^+}{(2P_2^+k_1^-+\mathbf{k}_{1T}^2)(2k_1^-k_2^++l_T^2)}+\mathcal{O}\left(\frac{\Lambda_{\rm QCD}}{m_B^2}\right)\right\},\end{aligned} \tag{18}$$

where the momenta are assigned in Fig. 3. The calculation from the second formula to the last one is approximated as $\langle k_1\rangle\ll\langle k_2\rangle$. This approximation is equal to taking the momenta of spectator quark in the B meson as $k_1=(0,k_1^-,\mathbf{k}_{1T})$. We neglect the last term which is a higher order one in terms of $1/m_B$ expansion. Therefore the integration of Eq. (5) is performed safely. Though we calculated the above factorization formulas by one order in terms of α_s, the radiative corrections at the next order would emerge in forms of $\alpha_s^2\ln(m/t)$, where m's denote some scales, i.e., m_B, $1/b,\ldots,$ in the hard part $H(t)$. Selecting t as the largest scale in m's, the largest logarithm in the next order corrections is killed. Accordingly, the scale t_i's in the above equations are chosen as

$$t_e^1=\max(\sqrt{x_2}m_B,1/b_1,1/b_2), \tag{19}$$

$$t_e^2=\max(\sqrt{x_1}m_B,1/b_1,1/b_2), \tag{20}$$

$$\begin{aligned}t_d&=\max(\sqrt{x_1x_2}m_B,\sqrt{x_2x_3}m_B,1/b_1,1/b_2),\\ t_f^1&=\max(\sqrt{x_2x_3}m_B,1/b_1,1/b_2),\\ t_f^2&=\max(\sqrt{x_2x_3}m_B,\sqrt{x_2+x_3-x_2x_3}m_B,1/b_1,1/b_2),\\ t_a&=\max(\sqrt{x_2}m_B,1/b_2,1/b_3).\end{aligned} \tag{21}$$

They are given the maximum values of the scales appearing in each diagram.

In the language of the above matrix elements for different diagrams Eqs. (13)–(17), the decay amplitude for $B^0\to\pi^+\pi^-$ can be written as

$$\begin{aligned}\mathcal{M}(B^0\to\pi^+\pi^-) &=f_\pi F_e\left[\xi_u\left(\frac{1}{3}C_1+C_2\right)-\xi_t\left(C_4+\frac{1}{3}C_3+C_{10}+\frac{1}{3}C_9\right)\right]\\ &\quad-f_\pi F_e^P\xi_t\left[C_6+\frac{1}{3}C_5+C_8+\frac{1}{3}C_7\right]\\ &\quad+\mathcal{M}_e[\xi_uC_1-\xi_t(C_3+C_9)]\\ &\quad+\mathcal{M}_a\left[\xi_uC_2-\xi_t\left(C_3+2C_4+2C_6+\frac{1}{2}C_8-\frac{1}{2}C_9+\frac{1}{2}C_{10}\right)\right]-f_BF_a\xi_t\left[\frac{1}{3}C_5+C_6-\frac{1}{6}C_7-\frac{1}{2}C_8\right],\end{aligned} \tag{22}$$

where $\xi_u=V_{ub}^*V_{ud}$, $\xi_t=V_{tb}^*V_{td}$. The decay width is expressed as

$$\Gamma=\frac{G_F^2m_B^3}{128\pi}|\mathcal{M}|^2. \tag{23}$$

The $C_i's$ should be calculated at the appropriate scale t_i using Eqs. (C1),(D1). The decay amplitude of the charge conjugate decay channel $\overline{B^0}\to\pi^+\pi^-$ is the same as Eq. (22)

except replacing the Cabibbo-Kobayashi-Maskawa (CKM) matrix elements ξ_u to ξ_u^* and ξ_t to ξ_t^* under the phase convention $CP|B^0\rangle=|\overline{B^0}\rangle$.

The decay amplitude for $B^0\to\pi^0\pi^0$ can be written as

$$\begin{aligned}
&-\sqrt{2}\mathcal{M}(B^0\to\pi^0\pi^0)\\
&\quad=f_\pi F_e\left[\xi_u\left(C_1+\frac{1}{3}C_2\right)+\xi_t\left(\frac{1}{3}C_3+C_4+\frac{3}{2}C_7+\frac{1}{2}C_8\right.\right.\\
&\quad\quad\left.\left.-\frac{5}{3}C_9-C_{10}\right)\right]+f_\pi F_e^P\xi_t\left[C_6+\frac{1}{3}C_5-\frac{1}{6}C_7-\frac{1}{2}C_8\right]\\
&\quad\quad+\mathcal{M}_e\left[\xi_uC_2-\xi_t\left(-C_3+\frac{3}{2}C_8+\frac{1}{2}C_9+\frac{3}{2}C_{10}\right)\right]\\
&\quad\quad-\mathcal{M}_a\left[\xi_uC_2-\xi_t\left(C_3+2C_4+2C_6+\frac{1}{2}C_8-\frac{1}{2}C_9\right.\right.\\
&\quad\quad\left.\left.+\frac{1}{2}C_{10}\right)\right]+f_BF_a\xi_t\left[\frac{1}{3}C_5+C_6-\frac{1}{6}C_7-\frac{1}{2}C_8\right].
\end{aligned}\tag{24}$$

The decay amplitude for $B^+\to\pi^+\pi^0$ can be written as

$$\begin{aligned}
&\sqrt{2}\mathcal{M}(B^+\to\pi^+\pi^0)\\
&\quad=f_\pi F_e\left[\frac{4}{3}\xi_u(C_1+C_2)-\xi_t\left(2C_{10}+2C_9-\frac{3}{2}C_7-\frac{1}{2}C_8\right)\right]\\
&\quad\quad-f_\pi F_e^P\xi_t\left[\frac{3}{2}C_8+\frac{1}{2}C_7\right]\\
&\quad\quad+\mathcal{M}_e\left[\xi_u(C_1+C_2)-\frac{3}{2}\xi_t(C_8+C_9+C_{10})\right].
\end{aligned}\tag{25}$$

From the above equations (22),(24),(25), it is easy to see that we have the exact Isospin relation for the three decays

$$\begin{aligned}
&\mathcal{M}(B^0\to\pi^+\pi^-)-\sqrt{2}\mathcal{M}(B^0\to\pi^0\pi^0)\\
&\quad=\sqrt{2}\mathcal{M}(B^+\to\pi^+\pi^0).
\end{aligned}\tag{26}$$

IV. NUMERICAL CALCULATIONS AND DISCUSSIONS OF RESULTS

In the numerical calculations we use [19]

$$\begin{gathered}
\Lambda_{\overline{\mathrm{MS}}}^{(f=4)}=0.25\ \mathrm{GeV},\quad f_\pi=0.13\ \mathrm{GeV},\quad f_B=0.19\ \mathrm{GeV},\\
M_B=5.2792\ \mathrm{GeV},\quad M_W=80.41\ \mathrm{GeV},\\
\tau_{B^\pm}=1.65\times10^{-12}\ \mathrm{s},\quad \tau_{B^0}=1.56\times10^{-12}\ \mathrm{s}
\end{gathered}\tag{27}$$

and

$$m_u=4.5\ \mathrm{MeV},\quad m_d=1.8m_u,\tag{28}$$

which is relevant to taking $m_0=1.5$ GeV. For the π wave function, we neglect the b dependence part, which is not important in numerical analysis. We use

$$\phi_\pi(x)=\frac{3}{\sqrt{2N_c}}f_\pi x(1-x)\{1+a^A[5(1-2x)^2-1]\},\tag{29}$$

with $a^A=0.8$, which is close to the Chernyak-Zhitnitsky (CZ) wave function [20]. For this axial vector wave function the asymptotic wave function [21], $a^A\sim0$, is suggested from QCD sum rules [22], diffractive dissociation of high momentum pions [23], the instanton model [24], and pion distribution functions [25], etc., but we adopt $a^A=0.8$ according to the discussion in Ref. [26]. ϕ_π' is chosen as asymptotic wave function

$$\phi_\pi'(x)=\frac{3}{\sqrt{2N_c}}f_\pi x(1-x)\{1+a^p[5(1-2x)^2-1]\},\tag{30}$$

with $a^P=0$. For B meson, the wave function is chosen as

$$\phi_B(x,b)=N_Bx^2(1-x)^2\exp\left[-\frac{M_B^2\ x^2}{2\omega_{b1}^2}-\frac{1}{2}(\omega_{b2}b)^2\right],\tag{31}$$

with $\omega_{b1}=\omega_{b2}=0.4$ GeV [27], and $N_B=91.745$ GeV is the normalization constant. In this work, we set $\omega_{b1}=\omega_{b2}$ for simplicity. We would like to point out that the choice of the meson wave functions as in Eqs. (29)–(31) and the above parameters cannot only explain the experimental data of $B\to\pi\pi$, but also $B\to K\pi$ [18,26], $D\pi$, etc., which is the result of a global fitting. However, since the predicted branching ratio of $B\to\pi\pi$ is sensitive to the input parameters f_B, m_0, a^A, a^P, and ω_{b1}, we will at first give the numerical results with the above parameters, then we give the allowed parameter regions of f_B, m_0, a^A, a^P, and ω_{b1} constrained by the experimental data of $B\to\pi^+\pi^-$ presented by CLEO.

The diagrams (a) and (b) in Fig. 3, calculated in Eq. (13) correspond to the $B\to\pi$ transition form factor $F^{B\pi}(q^2=0)$, where $q=p_B-P_2$. Our result is $F^{B\pi}(0)=0.25$ to be consistent with QCD sum rule one. This implies that PQCD can explain the transition form factor in the B meson decays, which is different from the conclusion in Ref. [12]. In that paper, because m_0 was not considered, perturbative contributions to $F^{B\pi}(0)$ were predicted to be much smaller than nonperturbative ones.

Although we take the CZ-like wave function ($a^A=0.8$) for ϕ_π, one finds that the above parameters give the pion electromagnetic form factor to be consistent with the experimental data. The pion electromagnetic form factor $F_\pi(Q^2)$ in PQCD is given as [28,29]

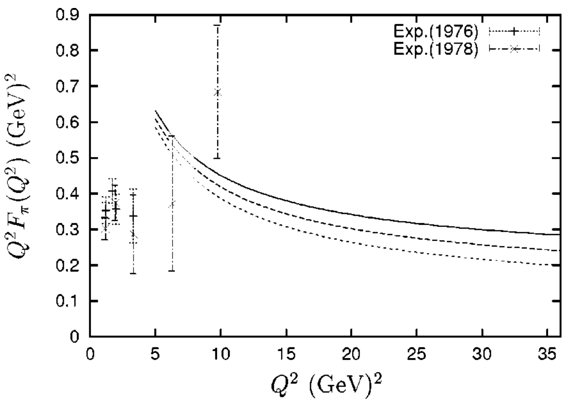

FIG. 4. Q^2 dependence for $F_\pi(Q^2)$ with the data [30]. The solid, dashed, and dotted lines correspond to $a^A=0.8,0.4$, and 0, respectively.

$$\begin{aligned}F_\pi(Q^2)=&16\pi C_F\int_0^1 dx_2dx_3\int_0^\infty b_2db_2\,b_3db_3\alpha_s(t)\\&\times h_e(x_3,x_2,b_3,b_2)\{x_2Q^2\phi_\pi(x_2,b_2)\phi_\pi(x_3,b_3)\\&+2m_0^2(1-x_2)\phi'_\pi(x_2,b_2)\phi'_\pi(x_3,b_3)\}\\&\times\exp[-S_\pi^1(t)-S_\pi^2(t)],\end{aligned}\tag{32}$$

where $-Q^2$ is the momentum transfer in this system, the scale t is chosen as $t=\max(\sqrt{x_2}Q,1/b_2,1/b_3)$, and m_B's are replaced by Q in the h_e,S_π^1 and S_π^2. One may suspect that around $x_1,x_2\sim 0$, the gluon and virtual quark propagators give rise to IR divergences which cannot be canceled by the wave functions. However, in PQCD, the transverse momenta k_T save perturbative calculations from the singularities around $x_{1,2}\sim 0$. There are still IR divergences around $k_T\sim 0$, but the Sudakov factor which can be calculated from QCD corrections does suppress such a region, i.e., nonperturbative contributions, sufficiently. We show the Q^2 dependence of $F_\pi(Q^2)$ [Eq. (32)] in Fig. 4 with the experimental data [30]. This figure shows that the parameters we used do not conflict with the data. We also show $F_\pi(Q^2)$ for $a^A=0.8,0.4$, and 0. It indicates that $F_\pi(Q^2)$ is fairly insensitive to a^A.

The CKM parameters we used here are

$$|V_{ud}|=0.9740\pm0.0010,\ \ |V_{ub}/V_{cb}|=0.08\pm0.02,\tag{33}$$

$$|V_{cb}|=0.0395\pm0.0017,\quad |V_{tb}^*V_{td}|=0.0084\pm0.0018.$$

We leave the CKM angle ϕ_2 as a free parameter. ϕ_2's definition is [31]

$$\phi_2=\arg\left[-\frac{V_{td}V_{tb}^*}{V_{ud}V_{ub}^*}\right].\tag{34}$$

In this parametrization, the decay amplitude of $B\to\pi\pi$ can be written as

$$\mathcal{M}=V_{ub}^*V_{ud}T-V_{tb}^*V_{td}P=V_{ub}^*V_{ud}T[1+ze^{i(\phi_2+\delta)}],\tag{35}$$

where $z=|V_{tb}^*V_{td}/V_{ub}^*V_{ud}||P/T|$, and δ is the relative strong phase between tree (T) diagrams and penguin diagrams (P). z and δ can be calculated from PQCD. For example, in $B^0\to\pi^+\pi^-$ decay, we get $z=30\%$, and $\delta=130°$, if we use the above parameters. Here in PQCD approach, the strong phases come from the nonfactorizable diagrams and annihilation type diagrams [see (c)–(h) in Fig. 3]. The internal quarks and gluons can be on mass shell providing the strong phases. This can also be seen from Eqs. (B8)–(B11), where the modified Bessel function $K_0(-if)$ has an imaginary part. Numerical analysis also shows that the main contribution to the relative strong phase δ comes from the annihilation diagrams, (g) and (h), in Fig. 3. From the figure, we can see that they are factorizable diagrams. B meson annihilates to $q\bar{q}$ quark pair and then decays to $\pi\pi$ final states. The intermediate $q\bar{q}$ quark pair represents a number of resonance states, which implies final state interaction. In perturbative calculations, the two quark lines can be cut providing the imaginary part. The importance of these diagrams also makes the contribution of penguin diagrams more important than previously expected.

This mechanism of producing CP violation strong phase is very different from the so-called Bander-Silverman-Soni (BSS) mechanism [32], where the strong phase comes from the perturbative penguin diagrams. The contribution of BSS mechanism to the direct CP violation in $B\to\pi^+\pi^-$ is only in the order of few percent [5,7]. It is higher order corrections (α_s suppressed) in our PQCD approach. Therefore in our approach we can safely neglect this contribution. The corresponding charge conjugate $\bar{B}$ decay is

$$\bar{\mathcal{M}}=V_{ub}V_{ud}^*T-V_{tb}V_{td}^*P=V_{ub}V_{ud}^*T[1+ze^{i(-\phi_2+\delta)}].\tag{36}$$

Therefore the averaged branching ratio for $B\to\pi\pi$ is

$$\begin{aligned}\mathrm{Br}&=(|\mathcal{M}|^2+|\bar{\mathcal{M}}|^2)/2\\&=|V_{ub}V_{ud}^*T|^2[1+2z\cos\phi_2\cos\delta+z^2].\end{aligned}\tag{37}$$

From this equation, we know that the averaged branching ratio is a function of CKM angle ϕ_2, if $z\cos\delta\neq 0$.

The averaged branching ratio of $B^0\to\pi^+\pi^-$ decay which is predicted from the formulas in the previous section is shown as a function of ϕ_2 in Fig. 5. To consider m_0 required from chiral symmetry is essentially different from the previous paper [11]. This figure shows that m_0 enhances the branching ratio to agree with the experimental data. There is a significant dependence on the CKM angle ϕ_2. The branching ratio of $B^0\to\pi^+\pi^-$ is larger when ϕ_2 is larger. The reason is that the penguin contribution is not small. The CLEO measured branching ratio of $B\to\pi^+\pi^-$ [6]

$$\mathrm{Br}(B\to\pi^+\pi^-)=(4.3^{+1.6}_{-1.4}\pm0.5)\times10^{-6},\tag{38}$$

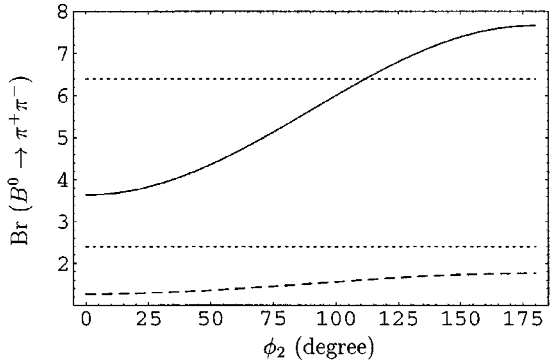

FIG. 5. Averaged branching ratios (in unit of 10^{-6}) of $B^0(\overline{B}^0) \to \pi^+\pi^-$, $m_0 = 1.5$ GeV (solid line), $m_0 = 0$ GeV (dashed line). The two dotted lines indicate the 1σ region of CLEO experiments in Eq. (38).

is in good agreement with our predictions. This prefers a lower value of ϕ_2. However, the predicted branching ratio is sensitive to the parameters of input. Especially it is sensitive to f_B, m_0 and the meson wave functions. Therefore, it is unlikely to use this single channel to determine the CKM angle ϕ_2.

The branching ratios of $B \to \pi\pi$ are sensitive to some input parameters. We give the parameter regions allowed by the experimental data in Eq. (38). Relevant parameters are m_0, a^P, and ω_{b1}. Others are specified in the beginning of this section. Here we check the sensitivity of our calculation on parameter m_0, a^P, and ω_{b1}. First we fix $m_0 = 1.5$ GeV and show the allowed region for a^P and ω_{b1}. This is shown in Fig. 6(a). One finds that the branching ratio is fairly insensitive to a^P. Second we fix $a^P = 0$ and show the allowed region for ω_{b1} and m_0. This is shown in Fig. 6(b). We see that the allowed region for ω_{b1} and m_0 is quite large. The dependence on a^A for the branching ratio of $B \to \pi^+\pi^-$ is given in Fig. 7. As discussed in Ref. [26], the central value of the experimental data $R_D = \mathrm{Br}(B^- \to D^0\pi^-)/\mathrm{Br}(\overline{B}_d^0 \to D^+\pi^-)$ requires $a^A = 0.8$, but this figure indicates that $B \to \pi^+\pi^-$ decay mode gives no significant restriction on a^A. Therefore, these figures show that the above set of parameters we choose for Fig. 5 is in the allowed region, and that parameter space producing the experimental data, Eq. (38), is quite large.

The branching ratio of $B^+ \to \pi^+\pi^0$ has little dependence on ϕ_2. It is easy to understand since there is only one dominant contribution from tree diagrams. The QCD penguin contribution is canceled by isospin relation and the electroweak contribution is very small giving only a slight dependence on ϕ_2. The branching ratio of this decay is predicted as 3×10^{-6}, using the parameters we list in the beginning of this section.

For the decay of $B^0 \to \pi^0\pi^0$, the situation is similar to that of $B^0 \to \pi^+\pi^-$. There are large contributions from both tree and penguin diagrams. We show the averaged branching ratio of $B^0 \to \pi^0\pi^0$ as a function of ϕ_2 in Fig. 8. Although the branching ratio is small, the dependence of ϕ_2 is significant. The predicted branching ratio of $B^0 \to \pi^0\pi^0$ is less than 10^{-6}. This is difficult for the B factories to measure the

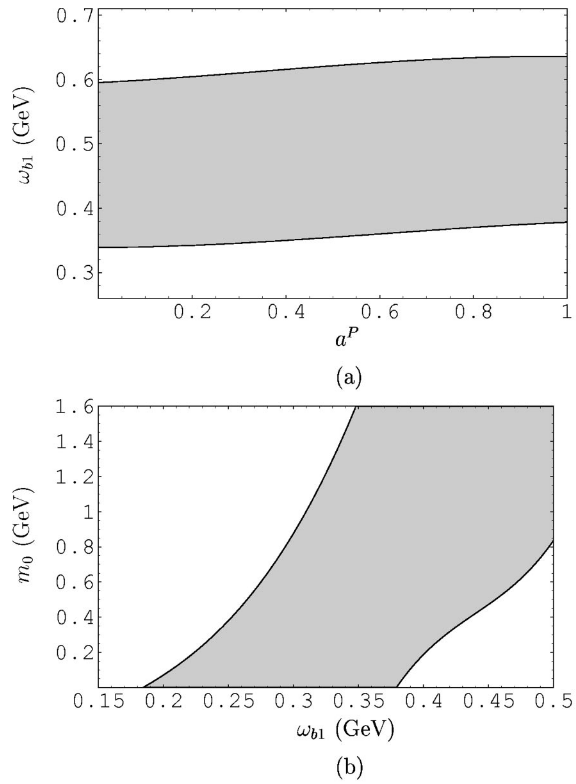

FIG. 6. Here we check the sensitivity of our calculation on parameter m_0, a^P, and ω_{b1}. Others are defined in the beginning of Sec. IV. The shaded areas are allowed by the data, Eq. (38), for arbitrary ϕ_2; (a) we fix $m_0 = 1.5$ GeV and show the region for a^P and ω_{b1}; (b) we fix $a^P = 0$ and show the allowed region for ω_{b1} and m_0.

separate branching ratios of B^0 and $\overline{B}^0$. In this case, the proposed isospin method to measure the CKM angle ϕ_2 [33] does not work in the B factories, since it requires the measurement of $B^0 \to \pi^0\pi^0$ and $\overline{B}^0 \to \pi^0\pi^0$.

Using Eqs. (35),(36), the direct CP violating parameter is

$$A_{CP}^{\mathrm{dir}} = \frac{|\mathcal{M}|^2 - |\overline{\mathcal{M}}|^2}{|\mathcal{M}|^2 + |\overline{\mathcal{M}}|^2} = \frac{-2z \sin\phi_2 \sin\delta}{1 + 2z\cos\phi_2 \cos\delta + z^2}. \quad (39)$$

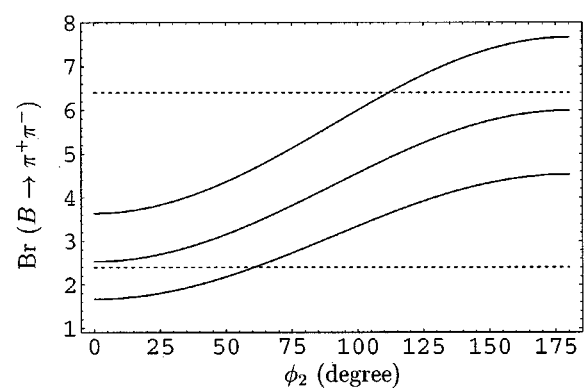

FIG. 7. Dependence on a^A for the branching ratio (in unit of 10^{-6}) of $B \to \pi^+\pi^-$. $a^A = 0.8, 0.4, 0$ in descending order, respectively.

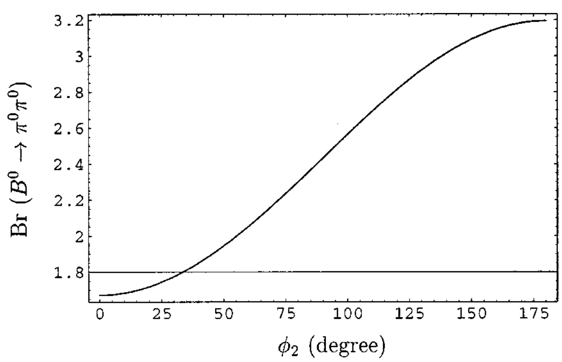

FIG. 8. Averaged branching ratios (in unit of 10^{-7}) of $B^0 \to \pi^0\pi^0$ as a function of CKM angle ϕ_2.

The direct CP asymmetry is nearly proportional to $\sin\phi_2$. We show the direct CP violation parameters (percentage) as a function of ϕ_2 in Fig. 9. Unlike the averaged branching ratios, the predicted CP violation in B decays does not depend much on the wave functions. They cancel each between the charge conjugate states shown in the above equation. The direct CP violation parameter of $B^0 \to \pi^+\pi^-$ and $\pi^0\pi^0$ can be as large as 40 and 20 % when ϕ_2 is near 70°. Because there is no annihilation diagram contribution in $B^+ \to \pi^+\pi^0$, the penguin contribution is negligible. The direct CP violation parameter of $B^+ \to \pi^+\pi^0$ is also very small. It is a horizontal line in Fig. 9.

For the neutral B^0 decays, there is more complication from the B^0-$\overline{B^0}$ mixing. The CP asymmetry is time dependent [5,34]:

$$A_{CP}(t) \simeq A_{CP}^{\rm dir} \cos(\Delta m t) + a_{\epsilon+\epsilon'} \sin(\Delta m t), \qquad (40)$$

where Δm is the mass difference of the two mass eigenstates of neutral B mesons. The direct CP violation parameter $A_{CP}^{\rm dir}$ is already defined in Eq. (39), while the mixing-related CP violation parameter is defined as

$$a_{\epsilon+\epsilon'} = \frac{-2\,\mathrm{Im}(\lambda_{CP})}{1+|\lambda_{CP}|^2}, \qquad (41)$$

where

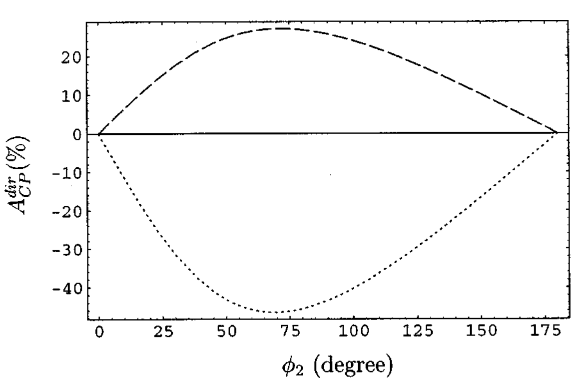

FIG. 9. Direct CP violation parameters (in percentage) of $B^0 \to \pi^+\pi^-$ (dotted line), and $B^+ \to \pi^+\pi^0$ (solid line), and $B^0 \to \pi^0\pi^0$ (dashed line) as a function of CKM angle ϕ_2.

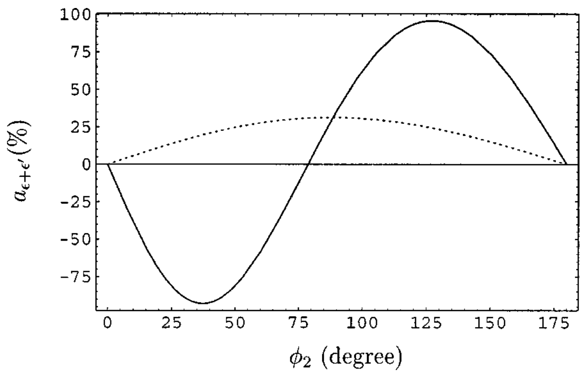

FIG. 10. CP violation parameters $a_{\epsilon+\epsilon'}$ (in percentage) of $B^0 \to \pi^+\pi^-$ (solid line), and $B^0 \to \pi^0\pi^0$ (dotted line), as a function of CKM angle ϕ_2.

$$\lambda_{CP} = \frac{V_{tb}^* V_{td} \langle f | H_{\rm eff} | \overline{B^0} \rangle}{V_{tb} V_{td}^* \langle f | H_{\rm eff} | B^0 \rangle}. \qquad (42)$$

Using Eqs. (35),(36), we can derive as

$$\lambda_{CP} = e^{2i\phi_2} \frac{1 + z e^{i(\delta-\phi_2)}}{1 + z e^{i(\delta+\phi_2)}}. \qquad (43)$$

Usually, people believe that the penguin diagram contribution is suppressed comparing with the tree contribution, i.e. $z \ll 1$, such that $\lambda_{CP} \simeq \exp[2i\phi_2]$, $a_{\epsilon+\epsilon'} = -\sin 2\phi_2$, and $A_{CP}^{\rm dir} \simeq 0$. That is the previous idea of extracting $\sin 2\phi_2$ from the CP measurement of $B^0 \to \pi^+\pi^-$. However, z is not very small. From Fig. 10, we can see that $a_{\epsilon+\epsilon'}$ is not a simple $-\sin 2\phi_2$ behavior due to the so-called penguin pollution.

If we integrate the time variable t, we will get the total CP asymmetry as

$$A_{CP} = \frac{1}{1+x^2} A_{CP}^{\rm dir} + \frac{x}{1+x^2} a_{\epsilon+\epsilon'}, \qquad (44)$$

with $x = \Delta m/\Gamma \simeq 0.723$ for the B^0-$\overline{B^0}$ mixing in SM [19]. The integrated CP asymmetries of $B^0 \to \pi^+\pi^-$ and $B^0 \to \pi^0\pi^0$ are shown in Fig. 11. Unlike the averaged branch-

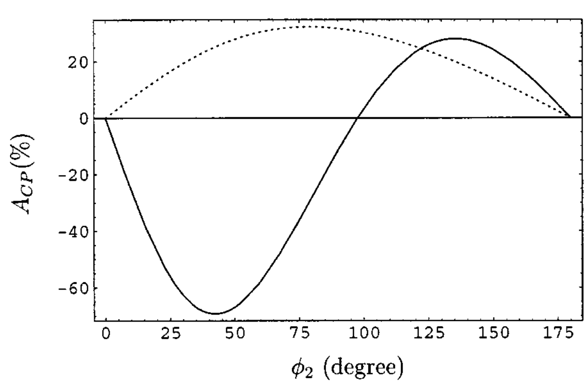

FIG. 11. The integrated CP asymmetries (in percentage) of $B^0 \to \pi^+\pi^-$ (solid line), and $B^0 \to \pi^0\pi^0$ (dotted line), as a function of CKM angle ϕ_2.

ing ratios, the CP asymmetry is not sensitive to the wave functions, since these parameter dependences canceled out. It is rather stable. If we can measure the integrated CP asymmetry from the experiments, then we can use this figure to determine the value of ϕ_2.

V. SUMMARY

We performed the calculations of $B^0\to\pi^+\pi^-$, $B^+\to\pi^+\pi^0$, and $B^0\to\pi^0\pi^0$ decays, in a perturbative QCD approach. In this approach, we calculate the nonfactorizable contributions and annihilation type contributions in addition to the usual factorizable contributions. The predicted branching ratios of $B^0\to\pi^+\pi^-$ are in good agreement with the experimental measurement by the CLEO Collaboration.

We found that the annihilation contributions were not as small as expected in a simple argument. The annihilation diagram, which provides the dominant strong phases, plays an important role in the CP violation asymmetries. We expect large direct CP asymmetries in the decay of $B^0\to\pi^+\pi^-$ and $B^0\to\pi^0\pi^0$. The ordinary method of measuring the CKM angle ϕ_2 will suffer from the large penguin pollution. The isospin method does not help, since the B factories cannot measure well the small branching ratio of $B^0\to\pi^0\pi^0$. Working in our PQCD approach, we give the predicted dependence of CP asymmetry on CKM angle ϕ_2. Using this dependence, the current running B factories in KEK and SLAC will be able to measure the CKM angle ϕ_2.

ACKNOWLEDGMENTS

We thank our PQCD group members Y.Y. Keum, E. Kou, T. Kurimoto, H.N. Li, T. Morozumi, A.I. Sanda, N. Sinha, R. Sinha, and T. Yoshikawa for helpful discussions. This work was supported by the Grant-in-Aid for Scientific Research on Priority Areas (Physics of CP violation). C.D.L. and M.Z.Y. thanks JSPS for support. K.U. thanks JSPS for partial support.

APPENDIX A: WILSON COEFFICIENTS

In this appendix we present the weak effective Hamiltonian $\mathcal{H}_{\rm eff}$ which we used to calculate the hard part $H(t)$ in Eq. (2). The $\mathcal{H}_{\rm eff}$ for the $\Delta B=1$ transitions at the scale smaller than m_W is given as

$$\mathcal{H}_{\rm eff}=\frac{G_F}{\sqrt{2}}\left[V_{ub}V_{ud}^*(C_1O_1^u+C_2O_2^u)-V_{tb}V_{td}^*\times\left(\sum_{i=3}^{10}C_i\,O_i+C_gO_g\right)\right]. \tag{A1}$$

We specify below the operators in $\mathcal{H}_{eff}$ for $b\to d$:

$$O_1^u=\overline{d}_\alpha\gamma^\mu Lu_\beta\cdot\overline{u}_\beta\gamma_\mu Lb_\alpha,\quad O_2^u=\overline{d}_\alpha\gamma^\mu Lu_\alpha\cdot\overline{u}_\beta\gamma_\mu Lb_\beta,$$

$$O_3=\overline{d}_\alpha\gamma^\mu Lb_\alpha\cdot\sum_{q'}\overline{q}'_\beta\gamma_\mu Lq'_\beta,$$

$$O_4=\overline{d}_\alpha\gamma^\mu Lb_\beta\cdot\sum_{q'}\overline{q}'_\beta\gamma_\mu Lq'_\alpha,$$

$$O_5=\overline{d}_\alpha\gamma^\mu Lb_\alpha\cdot\sum_{q'}\overline{q}'_\beta\gamma_\mu Rq'_\beta,$$

$$O_6=\overline{d}_\alpha\gamma^\mu Lb_\beta\cdot\sum_{q'}\overline{q}'_\beta\gamma_\mu Rq'_\alpha, \tag{A2}$$

$$O_7=\frac{3}{2}\overline{d}_\alpha\gamma^\mu Lb_\alpha\cdot\sum_{q'}e_{q'}\overline{q}'_\beta\gamma_\mu Rq'_\beta,$$

$$O_8=\frac{3}{2}\overline{d}_\alpha\gamma^\mu Lb_\beta\cdot\sum_{q'}e_{q'}\overline{q}'_\beta\gamma_\mu Rq'_\alpha,$$

$$O_9=\frac{3}{2}\overline{d}_\alpha\gamma^\mu Lb_\alpha\cdot\sum_{q'}e_{q'}\overline{q}'_\beta\gamma_\mu Lq'_\beta,$$

$$O_{10}=\frac{3}{2}\overline{d}_\alpha\gamma^\mu Lb_\beta\cdot\sum_{q'}e_{q'}\overline{q}'_\beta\gamma_\mu Lq'_\alpha.$$

Here α and β are the $SU(3)$ color indices; L and R are the left- and right-handed projection operators with $L=(1-\gamma_5)$, $R=(1+\gamma_5)$. The sum over q' runs over the quark fields that are active at the scale $\mu=O(m_b)$, i.e., $(q'\epsilon\{u,d,s,c,b\})$.

The PQCD approach works well for the leading twist approximation and leading double logarithm summation. For the Wilson coefficients, we will also use the leading logarithm summation for the QCD corrections, although the next-to-leading order calculations already exist in the literature [16]. This is the consistent way to cancel the explicit μ dependence in the theoretical formulas.

At m_W scale, the Wilson coefficients are evaluated for leading order as

$$C_{2w}=1,$$

$$C_{iw}=0,\quad i=1,8,10,$$

$$C_{3w}=-\frac{\alpha_s(m_W)}{24\pi}E_0+\frac{\alpha}{6\pi}\frac{1}{\sin^2\theta_W}(2B_0+C_0),$$

$$C_{4w}=\frac{\alpha_s(m_W)}{8\pi}E_0,$$

$$C_{5w}=-\frac{\alpha_s(m_W)}{24\pi}E_0,$$

$$C_{6w}=\frac{\alpha_s(m_W)}{8\pi}E_0,$$

$$C_{7w}=\frac{\alpha}{6\pi}(4C_0+D_0),$$

$$C_{9w}=\frac{\alpha}{6\pi}\left[4C_0+D_0+\frac{1}{\sin^2\theta_W}(10B_0-4C_0)\right], \tag{A3}$$

where

$$B_0=\frac{1}{4}\left(\frac{x}{1-x}+\frac{x}{(x-1)^2}\ln x\right),$$

$$C_0=\frac{x}{8}\left(\frac{x-6}{x-1}+\frac{3x+2}{(x-1)^2}\ln x\right),$$

$$D_0=-\frac{4}{9}\ln x+\frac{-19x^3+25x^2}{36(x-1)^3}+\frac{x^2(5x^2-2x-6)}{18(x-1)^4}\ln x,$$

$$E_0=-\frac{2}{3}\ln x+\frac{x(x^2+11x-18)}{12(x-1)^3}+\frac{x^2(4x^2-16x+15)}{6(x-1)^4}\ln x, \tag{A4}$$

with $x=m_t^2/m_W^2$.

If the scale $m_b<t<m_W$, then we evaluate the Wilson coefficients at t scale using leading logarithm running equations (C1). In numerical calculations, we use $\alpha_s=4\pi/[\beta_1\ln(t^2/\Lambda_{\rm QCD}^{(5)\,2})]$ which is the leading order expression with $\Lambda_{\rm QCD}^{(5)}=193$ MeV, derived from $\Lambda_{\rm QCD}^{(4)}=250$ MeV. Here $\beta_1=(33-2n_f)/3$, with the appropriate number of active quarks n_f. $n_f=5$ when scale t is larger than m_b.

The Wilson coefficients evaluated at $t=m_b=4.8$ GeV scale using the above equations are

$$\begin{aligned}
&C_1=-0.27034, \quad C_2=1.11879,\\
&C_3=0.01261, \quad C_4=-0.02695,\\
&C_5=0.00847, \quad C_6=-0.03260,\\
&C_7=0.00109, \quad C_8=0.00040,\\
&C_9=-0.00895, \quad C_{10}=0.00216.
\end{aligned} \tag{A5}$$

If the scale $t<m_b$, then we evaluate the Wilson coefficients at t scale using the input of Eq. (A5), and the formulas in Appendix D for four active quarks ($n_f=4$) (again in leading logarithm approximation).

APPENDIX B: FORMULAS FOR THE HARD PART CALCULATIONS

In this appendix we present the explicit expression of the formulas we used in Sec. III. First, we show the exponent $s(k,b)$ appearing in Eqs. (B4)–(B6). It is given, in terms of the variables

$$\hat{q}\equiv\ln(k/\Lambda), \quad \hat{b}\equiv\ln(1/b\Lambda) \tag{B1}$$

by

$$s(k,b)=\frac{2}{3\beta_1}\left[\hat{q}\ln\left(\frac{\hat{q}}{\hat{b}}\right)-\hat{q}+\hat{b}\right]+\frac{A^{(2)}}{4\beta_1^2}\left(\frac{\hat{q}}{\hat{b}}-1\right)-\left[\frac{A^{(2)}}{4\beta_1^2}-\frac{1}{3\beta_1}(2\gamma_E-1-\ln 2)\right]\ln\left(\frac{\hat{q}}{\hat{b}}\right). \tag{B2}$$

The above coefficients β_1 and $A^{(2)}$ are

$$\beta_1=\frac{33-2n_f}{12}$$

$$A^{(2)}=\frac{67}{9}-\frac{\pi^2}{3}-\frac{10}{27}n_f+\frac{8}{3}\beta_1\ln\left(\frac{e^{\gamma_E}}{2}\right), \tag{B3}$$

where γ_E is the Euler constant.

Note that s is defined for $\hat{q}\geqslant\hat{b}$, and set to zero for $\hat{q}<\hat{b}$. As a similar treatment, the complete Sudakov factor $\exp(-S)$ is set to unity, if $\exp(-S)>1$, in the numerical analysis. This corresponds to a truncation at large k_T, which spoils the on-shell requirement for the light valence quarks. The quark lines with large k_T should be absorbed into the hard scattering amplitude, instead of the wave functions.

$e^{-S_B(t)}$, $e^{-S_\pi^1(t)}$, and $e^{-S_\pi^2(t)}$ used in the amplitudes are expressions abbreviated to combine the Sudakov factor and single ultraviolet logarithms associated with the B and π meson wave functions. The exponents are defined as

$$S_B(t)=s(x_1m_B/\sqrt{2},b_1)-\frac{1}{\beta_1}\ln\frac{\ln(t/\Lambda)}{-\ln(b_1\Lambda)}, \tag{B4}$$

$$S_\pi^1(t)=s(x_2m_B/\sqrt{2},b_2)+s((1-x_2)m_B/\sqrt{2},b_2)-\frac{1}{\beta_1}\ln\frac{\ln(t/\Lambda)}{-\ln(b_2\Lambda)}, \tag{B5}$$

$$S_\pi^2(t)=s(x_3m_B/\sqrt{2},b_3)+s((1-x_3)m_B/\sqrt{2},b_3)-\frac{1}{\beta_1}\ln\frac{\ln(t/\Lambda)}{-\ln(b_3\Lambda)}. \tag{B6}$$

The last term of each equation is the integration result of the last term in Eq. (2).

The function h_i's, coming from the Fourier transform of hard part H, are given as

$$h_e(x_1,x_2,b_1,b_2)=K_0(\sqrt{x_1x_2}m_Bb_1)[\theta(b_1-b_2)K_0(\sqrt{x_2}m_Bb_1)I_0(\sqrt{x_2}m_Bb_2)+\theta(b_2-b_1)K_0(\sqrt{x_2}m_Bb_2)I_0(\sqrt{x_2}m_Bb_1)], \tag{B7}$$

$$h_d(x_1,x_2,x_3,b_1,b_2)=K_0(-i\sqrt{x_2x_3}m_Bb_2)[\theta(b_1-b_2)K_0(\sqrt{x_1x_2}m_Bb_1)I_0(\sqrt{x_1x_2}m_Bb_2)+\theta(b_2-b_1)\times K_0(\sqrt{x_1x_2}m_Bb_2)I_0(\sqrt{x_1x_2}m_Bb_1)], \tag{B8}$$

$$h_f^{(1)}(x_1,x_2,x_3,b_1,b_2)=K_0(-i\sqrt{x_2x_3}m_Bb_1)[\theta(b_1-b_2)K_0(-i\sqrt{x_2x_3}m_Bb_1)J_0(\sqrt{x_2x_3}m_Bb_2)+\theta(b_2-b_1)\times K_0(-i\sqrt{x_2x_3}m_Bb_2)J_0(\sqrt{x_2x_3}m_Bb_1)], \tag{B9}$$

$$h_f^{(2)}(x_1,x_2,x_3,b_1,b_2)=K_0(\sqrt{x_2+x_3-x_2x_3}m_Bb_1)[\theta(b_1-b_2)K_0(-i\sqrt{x_2x_3}m_Bb_1)J_0(\sqrt{x_2x_3}m_Bb_2)+\theta(b_2-b_1)\times K_0(-i\sqrt{x_2x_3}m_Bb_2)J_0(\sqrt{x_2x_3}m_Bb_1)], \tag{B10}$$

$$h_a(x_2,x_3,b_2,b_3)=K_0(-i\sqrt{x_2x_3}m_Bb_3)[\theta(b_2-b_3)K_0(-i\sqrt{x_2}m_Bb_2)J_0(\sqrt{x_2}m_Bb_3)+\theta(b_3-b_2)\times K_0(-i\sqrt{x_2}m_Bb_3)J_0(\sqrt{x_2}m_Bb_2)], \tag{B11}$$

with J_0 the Bessel function and K_0, I_0 modified Bessel functions $K_0(-ix)=-(\pi/2)Y_0(x)+i(\pi/2)J_0(x)$.

APPENDIX C: WILSON COEFFICIENTS RUNNING EQUATIONS ABOVE m_b SCALE

In this appendix, we list formulas for renormalization group running from m_W scale to t scale, where $t>m_b$. These formulas are derived from the leading logarithm QCD corrections with five active quarks [16]:

$$C_1=\frac{1}{2}(\eta^{-6/23}-\eta^{12/23}),$$

$$C_2=\frac{1}{2}(\eta^{-6/23}+\eta^{12/23}),$$

$$\begin{aligned}C_3=&0.0510\eta^{-0.4086}-0.0714\eta^{-6/23}+0.0054\eta^{-0.1456}-0.1403\eta^{0.4230}-0.0113\eta^{0.8994}+1/6\eta^{12/23}+C_{3w}(0.2868\eta^{-0.4086}\\&+0.0491\eta^{-0.1456}+0.6579\eta^{0.4230}+0.0061\eta^{0.8994})+C_{4w}(0.3287\eta^{-0.4086}+0.0424\eta^{-0.1456}-0.3263\eta^{0.4230}\\&-0.0448\eta^{0.8994})+C_{5w}(-0.0629\eta^{-0.4086}+0.1629\eta^{-0.1456}-0.1846\eta^{0.4230}+0.0846\eta^{0.8994})+C_{6w}(0.0447\eta^{-0.4086}\\&-0.0063\eta^{-0.1456}-0.2610\eta^{0.4230}+0.2226\eta^{0.8994})+C_{9w}(-0.0325\eta^{-0.4086}+0.0357\eta^{-6/23}-0.0016\eta^{-0.1456}\\&+0.2342\eta^{0.4230}-0.25\eta^{12/23}+0.0141\eta^{0.8994})+C_{7w}(-0.0063\eta^{-0.4086}+0.0163\eta^{-0.1456}-0.0185\eta^{0.4230}\\&+0.0085\eta^{0.8994}),\end{aligned}$$

$$\begin{aligned}C_4=&0.0984\eta^{-0.4086}-0.0714\eta^{-6/23}+0.0026\eta^{-0.1456}+0.1214\eta^{0.4230}-1/6\eta^{12/23}+0.0156\eta^{0.8994}+C_{3w}(0.5539\eta^{-0.4086}\\&+0.0239\eta^{-0.1456}-0.5693\eta^{0.4230}-0.0085\eta^{0.8994})+C_{4w}(0.6348\eta^{-0.4086}+0.0206\eta^{-0.1456}+0.2823\eta^{0.4230}\\&+0.0623\eta^{0.8994})+C_{5w}(-0.1215\eta^{-0.4086}+0.0793\eta^{-0.1456}+0.1597\eta^{0.4230}-0.1175\eta^{0.8994})+C_{6w}(0.0864\eta^{-0.4086}\\&-0.0031\eta^{-0.1456}+0.2259\eta^{0.4230}-0.3092\eta^{0.8994})+C_{9w}(-0.0627\eta^{-0.4086}+0.0357\eta^{-6/23}-0.0008\eta^{-0.1456}\\&-0.2027\eta^{0.4230}+0.25\eta^{12/23}-0.0196\eta^{0.8994})+C_{7w}(-0.0122\eta^{-0.4086}+0.0079\eta^{-0.1456}\\&+0.0160\eta^{0.4230}-0.0117\eta^{0.8994}),\end{aligned}$$

$$\begin{aligned}C_5=&-0.0397\eta^{-0.4086}+0.0304\eta^{-0.1456}+0.0117\eta^{0.4230}-0.0025\eta^{0.8994}+C_{3w}(-0.2233\eta^{-0.4086}+0.2767\eta^{-0.1456}\\&-0.0547\eta^{0.4230}+0.0013\eta^{0.8994})+C_{4w}(-0.2559\eta^{-0.4086}+0.2385\eta^{-0.1456}+0.0271\eta^{0.4230}-0.0098\eta^{0.8994})\\&+C_{5w}(0.0490\eta^{-0.4086}+0.9171\eta^{-0.1456}+0.0154\eta^{0.4230}+0.0185\eta^{0.8994})+C_{6w}(-0.0348\eta^{-0.4086}-0.0357\eta^{-0.1456}\\&+0.0217\eta^{0.4230}+0.0488\eta^{0.8994})+C_{9w}(0.0253\eta^{-0.4086}-0.0089\eta^{-0.1456}-0.0195\eta^{0.4230}+0.0031\eta^{0.8994})\\&+C_{7w}(0.0049\eta^{-0.4086}+0.0917\eta^{-0.1456}-0.1\eta^{-3/23}+0.0015\eta^{0.4230}+0.0019\eta^{0.8994}),\end{aligned}$$

$$
\begin{aligned}
C_6 = {} & 0.0335\eta^{-0.4086} - 0.0112\eta^{-0.1456} + 0.0239\eta^{0.4230} - 0.0462\eta^{0.8994} + C_{3w}(0.1885\eta^{-0.4086} - 0.1017\eta^{-0.1456} - 0.1120\eta^{0.4230} \\
& + 0.0251\eta^{0.8994}) + C_{4w}(0.2160\eta^{-0.4086} - 0.0877\eta^{-0.1456} + 0.0555\eta^{0.4230} - 0.1839\eta^{0.8994}) + C_{5w}(-0.0414\eta^{-0.4086} \\
& - 0.3370\eta^{-0.1456} + 0.0314\eta^{0.4230} + 0.3469\eta^{0.8994}) + C_{6w}(0.0294\eta^{-0.4086} + 0.0131\eta^{-0.1456} + 0.0444\eta^{0.4230} \\
& + 0.9131\eta^{0.8994}) + C_{9w}(-0.0213\eta^{-0.4086} + 0.0033\eta^{-0.1456} - 0.0399\eta^{0.4230} + 0.0579\eta^{0.8994}) + C_{7w}(-0.0041\eta^{-0.4086} \\
& - 0.0337\eta^{-0.1456} + \eta^{-3/23}/30 + 0.0031\eta^{0.4230} + 0.0347\eta^{0.8994} - \eta^{24/23}/30), \\
C_7 = {} & C_{7w}\eta^{-3/23}, \\
C_8 = {} & \frac{1}{3}C_{7w}(-\eta^{-3/23} + \eta^{24/23}), \\
C_9 = {} & \frac{1}{2}C_{9w}(\eta^{-6/23} + \eta^{12/23}), \\
C_{10} = {} & \frac{1}{2}C_{9w}(\eta^{-6/23} - \eta^{12/23}),
\end{aligned}
\tag{C1}
$$

where $\eta = \alpha_s(t)/\alpha_s(m_W)$.

APPENDIX D: WILSON COEFFICIENTS RUNNING EQUATIONS BELOW m_b SCALE

In this appendix, we list formulas for renormalization group running from m_b scale to t scale, where $t < m_b$. These formulas are derived from the leading logarithm QCD corrections with four active quarks [16].

$$
\begin{aligned}
CC_1 = {} & \frac{1}{2}C_2(\zeta^{-6/25} - \zeta^{12/25}) + \frac{1}{2}C_1(\zeta^{-6/25} + \zeta^{12/25}), \\
CC_2 = {} & \frac{1}{2}C_2(\zeta^{-6/25} + \zeta^{12/25}) + \frac{1}{2}C_1(\zeta^{-6/25} - \zeta^{12/25}), \\
CC_3 = {} & C_4(0.3606\zeta^{-0.3469} + 0.03166\zeta^{-0.1317} - 0.3626\zeta^{0.4201} - 0.0297\zeta^{0.8451}) + C_{10}(0.0149\zeta^{-0.3469} - 0.0020\zeta^{-0.1317} \\
& - 0.4981\zeta^{0.4201} + 0.5\zeta^{12/25} - 0.0148\zeta^{0.8451}) + C_2(0.0651\zeta^{-0.3469} - 0.0833\zeta^{-6/25} + 0.0046\zeta^{-0.1317} - 0.2265\zeta^{0.4201} \\
& + 0.25\zeta^{12/25} - 0.0099\zeta^{0.8451}) + C_3(0.3308\zeta^{-0.3469} + 0.0356\zeta^{-0.1317} + 0.6337\zeta^{0.4201} - 0.0001\zeta^{0.8451}) \\
& + C_1(0.0502\zeta^{-0.3469} - 0.0833\zeta^{-6/25} + 0.0066\zeta^{-0.1317} + 0.2717\zeta^{0.4201} - 0.25\zeta^{12/25} + 0.0049\zeta^{0.8451}) \\
& + C_9(-0.0149\zeta^{-0.3469} + 0.0020\zeta^{-0.1317} + 0.4981\zeta^{0.4201} - 0.5\zeta^{12/25} + 0.0148\zeta^{0.8451}) \\
& + C_5(-0.0598\zeta^{-0.3469} + 0.1371\zeta^{-0.1317} - 0.1473\zeta^{0.4201} + 0.0700\zeta^{0.8451}) \\
& + C_6(0.0377\zeta^{-0.3469} - 0.0045\zeta^{-0.1317} - 0.2210\zeta^{0.4201} + 0.18775\zeta^{0.8451}) \\
& + C_7(-0.0150\zeta^{-0.3469} + 0.0343\zeta^{-0.1317} - 0.0368\zeta^{0.4201} + 0.0175\zeta^{0.8451}) + C_8(0.009\zeta^{-0.3469} - 0.0011\zeta^{-0.1317} \\
& - 0.0553\zeta^{0.4201} + 0.0469\zeta^{0.8451}), \\
CC_4 = {} & C_6(0.0640\zeta^{-0.3469} - 0.0021\zeta^{-0.1317} + 0.2018\zeta^{0.4201} - 0.2637\zeta^{0.8451}) + C_5(-0.10156\zeta^{-0.3469} + 0.06538\zeta^{-0.1317} \\
& + 0.1345\zeta^{0.4201} - 0.09836\zeta^{0.8451}) + C_9(-0.02528\zeta^{-0.3469} + 0.0009\zeta^{-0.1317} - 0.4549\zeta^{0.4201} + 0.5\zeta^{12/25} - 0.0207\zeta^{0.8451}) \\
& + C_1(0.08515\zeta^{-0.3469} - 0.0833\zeta^{-6/25} + 0.0031\zeta^{-0.1317} - 0.24809\zeta^{0.4201} + 0.25\zeta^{12/25} - 0.00688\zeta^{0.8451}) \\
& + C_3(0.5615\zeta^{-0.3469} + 0.01699\zeta^{-0.1317} - 0.5787\zeta^{0.4201} + 0.0002\zeta^{0.8451}) + C_2(0.1104\zeta^{-0.3469} - 0.0833\zeta^{-6/25} \\
& + 0.0022\zeta^{-0.1317} + 0.2068\zeta^{0.4201} - 0.25\zeta^{12/25} + 0.0139\zeta^{0.8451}) + C_{10}(0.0253\zeta^{-0.3469} - 0.0009\zeta^{-0.1317} + 0.4549\zeta^{0.4201} \\
& - 0.5\zeta^{12/25} + 0.0207\zeta^{0.8451}) + C_4(0.6121\zeta^{-0.3469} + 0.0151\zeta^{-0.1317} + 0.3311\zeta^{0.4201} + 0.0417\zeta^{0.8451}) + C_8(0.0160\zeta^{-0.3469} \\
& - 0.0005\zeta^{-0.1317} + 0.0505\zeta^{0.4201} - 0.0659\zeta^{0.8451}) + C_7(-0.0254\zeta^{-0.3469} + 0.0163\zeta^{-0.1317} + 0.0336\zeta^{0.4201}
\end{aligned}
$$

$$-0.0246\zeta^{0.8451}),$$

$$CC_5=C_4(-0.2291\zeta^{-0.3469}+0.2167\zeta^{-0.1317}+0.0192\zeta^{0.4201}-0.0067\zeta^{0.8451})+C_{10}(-0.0095\zeta^{-0.3469}-0.0136\zeta^{-0.1317}$$
$$+0.0264\zeta^{0.4201}-0.0034\zeta^{0.8451})+C_2(-0.0413\zeta^{-0.3469}+0.0316\zeta^{-0.1317}+0.0120\zeta^{0.4201}-0.0022\zeta^{0.8451})$$
$$+C_3(-0.2102\zeta^{-0.3469}+0.2438\zeta^{-0.1317}-0.0336\zeta^{0.4201})+C_1(-0.0319\zeta^{-0.3469}+0.0452\zeta^{-0.1317}-0.0144\zeta^{0.4201}$$
$$+0.0011\zeta^{0.8451})+C_9(0.0095\zeta^{-0.3469}+0.0136\zeta^{-0.1317}-0.0264\zeta^{0.4201}+0.0034\zeta^{0.8451})+C_5(0.0380\zeta^{-0.3469}$$
$$+0.9382\zeta^{-0.1317}+0.0078\zeta^{0.4201}+0.0159\zeta^{0.8451})+C_6(-0.0240\zeta^{-0.3469}-0.0305\zeta^{-0.1317}+0.0117\zeta^{0.4201}$$
$$+0.0427\zeta^{0.8451})+C_8(-0.0060\zeta^{-0.3469}-0.0076\zeta^{-0.1317}+0.0029\zeta^{0.4201}+0.0107\zeta^{0.8451})+C_7(0.0095\zeta^{-0.3469}$$
$$+0.2346\zeta^{-0.1317}-0.25\zeta^{-3/25}+0.0020\zeta^{0.4201}+0.0040\zeta^{0.8451}),$$

$$CC_6=C_4(0.1825\zeta^{-0.3469}-0.0784\zeta^{-0.1317}+0.0449\zeta^{0.4201}-0.14894\zeta^{0.8451})+C_{10}(0.0075\zeta^{-0.3469}+0.0049\zeta^{-0.1317}$$
$$+0.0617\zeta^{0.4201}-0.07412\zeta^{0.8451})+C_2(0.0329\zeta^{-0.3469}-0.0114\zeta^{-0.1317}+0.0280\zeta^{0.4201}-0.0495\zeta^{0.8451})$$
$$+C_3(0.1674\zeta^{-0.3469}-0.0882\zeta^{-0.1317}-0.0784\zeta^{0.4201}-0.0007\zeta^{0.8451})+C_1(0.0254\zeta^{-0.3469}-0.0163\zeta^{-0.1317}$$
$$-0.0336\zeta^{0.4201}+0.0246\zeta^{0.8451})+C_9(-0.0075\zeta^{-0.3469}-0.0049\zeta^{-0.1317}-0.0617\zeta^{0.4201}+0.07412\zeta^{0.8451})$$
$$+C_5(-0.0303\zeta^{-0.3469}-0.3395\zeta^{-0.1317}+0.0182\zeta^{0.4201}+0.35157\zeta^{0.8451})+C_6(0.0191\zeta^{-0.3469}+0.0110\zeta^{-0.1317}$$
$$+0.0274\zeta^{0.4201}+0.94253\zeta^{0.8451})+C_8(0.0048\zeta^{-0.3469}+0.0028\zeta^{-0.1317}+0.0068\zeta^{0.4201}+0.2356\zeta^{0.8451}-0.25\zeta^{24/25})$$
$$+C_7(-0.0076\zeta^{-0.3469}-0.0849\zeta^{-0.1317}+0.0833\zeta^{-3/25}+0.0046\zeta^{0.4201}+0.0879\zeta^{0.8451}-0.0833\zeta^{24/25}),$$

$$CC_7=C_7\zeta^{-3/25},$$

$$CC_8=C_7(-\zeta^{-3/25}+\zeta^{24/25})/3.+C_8\zeta^{24/25},$$

$$CC_9=C_{10}(0.5\zeta^{-6/25}-0.5\zeta^{12/25})+C_9(0.5\zeta^{-6/25}+0.5\zeta^{12/25}),$$

$$CC_{10}=C_9(0.5\zeta^{-6/25}-0.5\zeta^{12/25})+C_{10}(0.5\zeta^{-6/25}+0.5\zeta^{12/25}), \tag{D1}$$

where $\zeta=\alpha_s(t)/\alpha_s(m_B)$. Here $\Lambda_{\rm QCD}^{(4)}=250$ MeV.

[1] See, for example, I. I. Bigi and A. I. Sanda, *CP Violation* (Cambridge University Press, Cambridge, England, 2000).
[2] M. Wirbel, B. Stech, and M. Bauer, Z. Phys. C **29**, 637 (1985); M. Bauer, B. Stech, and M. Wirbel, *ibid.* **34**, 103 (1987); L.-L. Chau, H.-Y. Cheng, W. K. Sze, H. Yao, and B. Tseng, Phys. Rev. D **43**, 2176 (1991); **58**, 019902 (1998).
[3] A. Ali, G. Kramer, and C. D. Lü, Phys. Rev. D **58**, 094009 (1998); C. D. Lü, Nucl. Phys. B (Proc. Suppl.) **74**, 227 (1999).
[4] Y.-H. Chen, H.-Y. Cheng, B. Tseng, and K.-C. Yang, Phys. Rev. D **60**, 094014 (1999); H.-Y. Cheng and K.-C. Yang, *ibid.* **62**, 054029 (2000).
[5] A. Ali, G. Kramer, and C. D. Lü, Phys. Rev. D **59**, 014005 (1999); C. D. Lu, invited talk at ''3rd International Conference on *B* Physics and *CP* Violation (BCONF99),'' Taipei, Taiwan, 1999, hep-ph/0001321.
[6] CLEO Collaboration, D. Cronin-Hennessy *et al.*, hep-ex/0001010.
[7] M. Beneke, G. Buchalla, M. Neubert, and C. T. Sachrajda, Phys. Rev. Lett. **83**, 1914 (1999).
[8] H. N. Li and H. L. Yu, Phys. Rev. Lett. **74**, 4388 (1995); Phys. Lett. B **353**, 301 (1995); H.-n. Li, *ibid.* **348**, 597 (1995); H. N. Li and H. L. Yu, Phys. Rev. D **53**, 2480 (1996).
[9] H.-n. Li and B. Tseng, Phys. Rev. D **57**, 443 (1998).
[10] See third reference in [8].
[11] M. Dahm, R. Jakob, and P. Kroll, Z. Phys. C **68**, 595 (1995).
[12] T. Feldmann and P. Kroll, Eur. Phys. J. C **12**, 99 (2000).
[13] C. H. Chang and H. N. Li, Phys. Rev. D **55**, 5577 (1997); T. W. Yeh and H. N. Li, *ibid.* **56**, 1615 (1997).
[14] G. P. Lepage and S. Brodsky, Phys. Rev. D **22**, 2157 (1980).
[15] J. Botts and G. Sterman, Nucl. Phys. **B225**, 62 (1989).
[16] For a review, see G. Buchalla, A. J. Buras, and M. E. Lautenbacher, Rev. Mod. Phys. **68**, 1125 (1996).
[17] H. N. Li, Phys. Rev. D **52**, 3958 (1995).
[18] Y. Y. Keum, H.-n. Li, and A. I. Sanda, Report No. KEK-TH-642, NCKU-HEP-00-01, hep-ph/0004004.
[19] Particle Data Group, C. Caso *et al.*, Eur. Phys. J. C **3**, 1 (1998).
[20] V. L. Chernyak and A. R. Zhitnitsky, Phys. Rep. **112**, 173 (1984).
[21] P. Kroll and M. Raulfs, Phys. Lett. B **387**, 848 (1996); S. J.

Brodsky, C. R. Ji, A. Pang, and D. G. Robertson, Phys. Rev. D **57**, 245 (1998); I. V. Musatov and A. V. Radyushkin, *ibid.* **56**, 2713 (1997).

[22] A. P. Bakulev and S. V. Mikhailov, Mod. Phys. Lett. A **11**, 1611 (1996); V. Braun and I. Halperin, Phys. Lett. B **328**, 457 (1994).

[23] E791 Collaboration, D. Ashery, hep-ex/9910024.

[24] V. Y. Petrov, M. V. Polyakov, R. Ruskov, C. Weiss, and K. Goeke, Phys. Rev. D **59**, 114018 (1999).

[25] T. Huang, B.-Q. Ma, and Q.-X. Shen, Phys. Rev. D **49**, 1490 (1994); F.-G. Cao, T. Huang, and B.-Q. Ma, *ibid.* **53**, 6582 (1996); R. Jakob, P. Kroll, and M. Raulfs, J. Phys. G **22**, 45 (1996).

[26] Y. Y. Keum, H.-n. Li, and A. I. Sanda, hep-ph/0004173.

[27] M. Bauer and M. Wirbel, Z. Phys. C **42**, 671 (1989).

[28] B. V. Geshkenbein and M. V. Terentev, Phys. Lett. **117B**, 243 (1982).

[29] A. I. Sanda and K. Ukai (in preparation).

[30] C. J. Bebek *et al.*, Phys. Rev. D **13**, 25 (1976); **17**, 1693 (1978).

[31] J. L. Rosner, A. I. Sanda, and M. P. Schmidt, in *Proceedings of the Workshop on High Sensitivity Beauty Physics*, Batavia, 1987, edited by A. J. Slaughter, N. Lockyer, and M. Schmidt (Fermilab, Batavia, 1987), p. 165; C. Hamzaoui, J. L. Rosner, and A. I. Sanda, *ibid.*, p. 215.

[32] M. Bander, D. Silverman, and A. Soni, Phys. Rev. Lett. **43**, 242 (1979).

[33] M. Gronau and D. London, Phys. Rev. Lett. **65**, 3381 (1990).

[34] G. Kramer, W. F. Palmer, and Y. L. Wu, Commun. Theor. Phys. **27**, 457 (1997).